# Spatially-constrained growth enhances conversional meltdown

Maxim O. Lavrentovich,[1,*] Mary E. Wahl,[2] Andrew W. Murray,[2,3] and David R. Nelson[2,4]

[1] *Department of Physics & Astronomy, University of Pennsylvania, Philadelphia, PA 19104, USA*
[2] *Department of Molecular & Cellular Biology, Harvard University, Cambridge, MA 02138, USA*
[3] *FAS Center for Systems Biology, Harvard University, Cambridge, MA 02138, USA*
[4] *Department of Physics, Harvard University, Cambridge, MA 02138, USA*

(Dated: June 25, 2015)

Cells that mutate or commit to a specialized function (differentiate) often undergo conversions that are effectively irreversible. Slowed growth of converted cells can act as a form of selection, balancing unidirectional conversion to maintain both cell types at a steady-state ratio. When conversion is insufficiently counterbalanced by selection, the original cell type will ultimately be lost, often with negative impacts on the population's fitness. The critical relationship between selection and conversion for maintenance of unconverted cells and the ratio between cell types at steady state (if one exists) depend on the spatial circumstances under which cells proliferate. We present analytical predictions for growth in several biologically-relevant geometries – well-mixed liquid media, radially-expanding colonies on flat surfaces, and linear fronts – by employing analogies to the directed percolation transition from non-equilibrium statistical physics. We test these predictions *in vivo* using a yeast strain engineered to undergo irreversible conversion: this synthetic system permits cell type-specific fluorescent labeling and exogenous variation of the relative growth and conversion rates. We find that populations confined to grow on a surface are more susceptible to fitness loss via a conversion-induced "meltdown."

## INTRODUCTION

Irreversible change is an important aspect of both development [1] and evolution [2]. Many mature tissues retain stem cells that replenish specialized cells lost to damage or aging. Proliferation counterpoised by irreversible differentiation can maintain stem and specialized cells in a dynamic steady-state [3], but an imbalance between these forces can eliminate the stem cell population, with dire health consequences [4]. Like differentiation, harmful mutations can be effectively irreversible; natural selection may check their spread due mutant organisms' slower reproduction, but if the mutation rate is too great or selection ineffectual, these mutations can fix permanently as described for mutational meltdown via Muller's ratchet [5, 6]. We will employ the generic term "conversional meltdown" to describe the loss of an unconverted cell type due to improper balance between mutation and selection, differentiation and proliferation, and, more generally, any form of irreversible conversion and differential growth. The abrupt shift from maintenance to extinction of the unconverted cell type as conversion rate increases is analogous to the well-studied directed percolation phase transition in statistical physics [7, 8].

Though most analyses of this phase transition have focussed on well-mixed populations, it is becoming clear that spatial structure plays a crucial role [9, 10]. Here, we investigate the phase transition for one-dimensional growth without migration, a geometry relevant in natural circumstances such as population expansion and growth of plant meristem, as well as in experimentally-tractable systems such as microbial range expansions [11, 12]. Yeast [12] and immotile bacteria [11] on Petri dishes grow in colonies that remain relatively flat, proliferating primarily at the edges [13] due to nutrient depletion in the core: the thin region of dividing cells at the frontier can thus be treated as a one-dimensional population. The interior of the colony accurately reflects the appearance of this population in the past; its composition can be studied using fluorescence detection techniques. When a particular cell type has locally fixed at the colony frontier, its descendants form a "sector" as shown in blue in Fig. 1(a). The geometric properties of the spatial sectors reflect the underlying evolutionary dynamics: for example, the sector opening angle $\theta$ provides an estimate of the selective advantage of cells in the sector relative to their neighbors [12].

Here we investigate the effect of spatial population structure on the conversional meltdown phase transition. We complement analytical and simulation-based approaches with *in vivo* validation of our predictions. We employ a strain of budding yeast engineered to undergo irreversible conversions with tunable frequency and fitness cost to study population dynamics in well-mixed liquid media, as well as microbial range expansions on Petri dishes. We find that the spatial distribution of the cells qualitatively changes the dynamics. Only adjacent individuals in spatially distributed populations will compete and the local effective population size will be small relative to the total population. The small number of competing individuals induces small number fluctuations or genetic drift. We will show through experiments, simulation, and theory that the enhanced genetic drift drives extinction. This has important consequences for diverse processes including tissue renewal, meristematic growth, and mutation-selection balance, where proliferation must occur faster than expected to prevent extinction of the unconverted population.

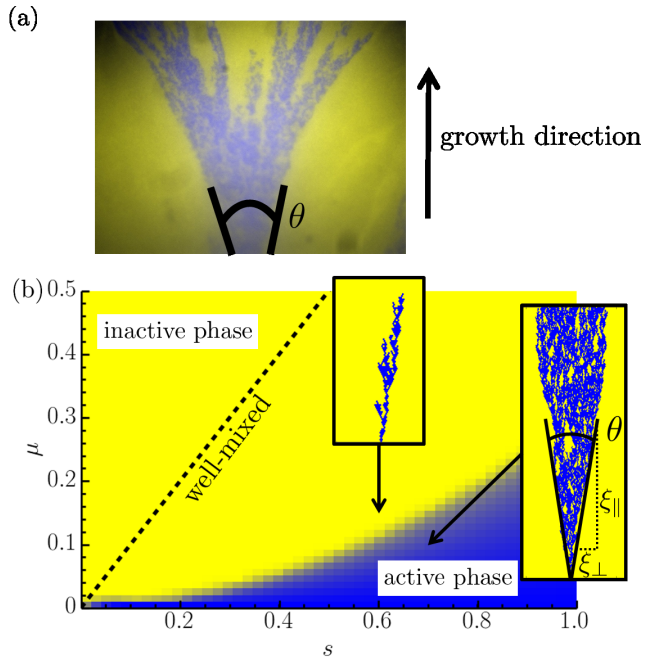


FIG. 1. (a) A micrograph of the edge of a budding yeast *S. cerevisiae* cell colony grown on a Petri dish. In this yeast range expansion, the blue unconverted cells form a spatial sector with an opening angle $\theta$ marked with overlayed black lines. The blue cells may convert to the yellow ones at a rate $\mu$, which leaves yellow patches within the blue sector. The growth, or time-like, direction is indicated. (b) A phase diagram indicating where we expect the extinction of the blue strain as a function of its selective advantage $s$ and conversion rate $\mu$. In the inactive phase, a genetic sector formed by a blue cell always dies out. In the active phase, there is a non-zero probability of forming a surviving cluster. The insets show examples of simulated sectors. Note the resemblance between the sector in the active phase and the experimental sector in part (a).

## EXPERIMENTAL SETUP

Microbes such as the budding yeast, *S. cerevisiae*, are easily cultured in both test tubes and on Petri dishes. This makes them excellent candidates for comparing well-mixed and spatial dynamics. Construction of a yeast strain which undergoes irreversible conversion events with exogenously-tunable conversion rates and fitness cost was described in Ref. [14]. Briefly, we genetically engineered an *S. cerevisiae* strain to lose a cycloheximide resistant ribosomal protein coding sequence via a $\beta$-estradiol-dependent Cre recombinase mechanism developed by Lindstrom et al. [15]. This irreversible conversion event occurs once per cell division (during mitotic exit) with a probability $\mu$, which we will call the conversion or mutation rate (per division). The probability $\mu$ depends on the ambient $\beta$-estradiol concentration. The cycloheximide resistant sequence (the *cyh2*$^r$ allele of the ribosomal protein L28 [16]) confers a measurable selective advantage for the unconverted strain relative to the converted strain when the strains are grown in the presence of cycloheximide. The selection coefficient $s \geq 0$ associated with this advantage is tunable by varying the cycloheximide concentration. Both the conversion rate $\mu$ and selection coefficient $s$ can be directly measured in well-mixed media and tuned over more than an order of magnitude by selecting appropriate $\beta$-estradiol and cycloheximide concentrations. Since these compounds are not consumed by the cells and diffuse readily through agar, and because yeast colonies are not particularly thick, these measurements also reflect $\mu$ and $s$ for populations grown on agar media.

To measure the fraction of converted versus unconverted cells in the population over time, we labeled the two types with fluorescent markers. Specifically, the coding sequence for the fluorescent protein mCherry is excised along with *cyh2*$^r$ via the Cre recombinase mechanism. After the recombination event, an mCitrine fluorescent protein is expressed, instead. This allows us to monitor the unconverted and converted cells using two different fluorescence channels. Throughout this manuscript, we will color the unconverted, mCherry-expressing cells blue and the converted, mCitrine-expressing cells yellow (Fig. 1(a), for example).

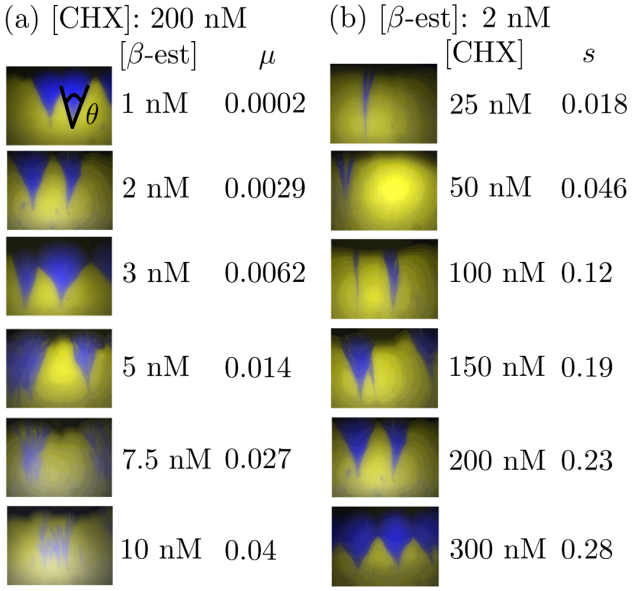


FIG. 2. Edges of linear range expansions under different growth conditions. In (a), the $\beta$-estradiol concentration in the agar is varied with a fixed cycloheximide concentration. The corresponding conversion rates $\mu$ are indicated. In the top-most panel, we indicate an opening sector angle. In (b), the cycloheximide concentration is varied instead, tuning the selective advantage $s$ of the blue strain over the yellow over a broad range. Note that the sector angles get smaller as we either increase $\mu$ or decrease $s$ and approach the directed percolation (conversional meltdown) transition.

To visualize the directed percolation phase transition or conversional meltdown, we produced linear range expansions on 1% agar media with judiciously-chosen $\beta$-estradiol and cycloheximide concentrations. To initiate the expansion, a thin strip of Whatman filter paper was submerged in a mixture of unconverted and converted cells, then placed in the center of the Petri dish; the linear colonies were then imaged after seven days' growth ($\approx 1$ cm) at 30 °C. The ratio of unconverted to converted cells in the inoculum was chosen to be small enough so that resulting sectors of unconverted cells would typically be sufficiently separated for analysis. Fig. 2 displays representative images for colonies grown in a variety of agar media, the concentrations of $\beta$-estradiol and cycloheximide used in each, and the corresponding $\mu$ and $s$ values. The different preparations influence the range expansion dynamics: we see that either increasing $\beta$-estradiol concentrations or decreasing cycloheximide will yield smaller blue sectors in Fig. 2, indicating an approach to extinction of the unconverted blue strain. We will also consider range expansions in which we place a droplet of the yeast cell solution at the center of the Petri dish, which then forms a circular colony that spreads out radially.

Thus, we are able to manipulate $\mu$ and $s$ in experiment by varying the concentrations of $\beta$-estradiol and cycloheximide, respectively, in either the nutrient medium for well-mixed populations grown in test-tube, or in the agar for populations grown on plates. Note that it is possible to vary $\mu$ and $s$ over a large range, covering the range of values in the simulated phase diagram in Fig. 1(b): in particular, we are able to tune through the transition line and see extinction of the unconverted strain. We will now theoretically analyze this transition line and the extinction in more detail.

## THEORY AND SIMULATION

The interior of the yeast colony or range expansion will be shielded from nutrients [13] and the frontier will be relatively thin, allowing us to approximate it as a one-dimensional population [8]. Then, provided the yeast colony experiences an effective surface tension that forces the colony boundary to remain uniform, we may consider the dynamics along a uniform, effectively one-dimensional flat front. Consider the fraction $f(x,t)$ of blue cells along the frontier at position $x$ and time $t$. Every generation time $\tau_g$, the fraction $f(x,t)$ will change due to the conversion probability $\mu$ and the competition at the frontier (which will depend on the selection coefficient $s$). For small $s$ and $\mu$, the fraction $f(x,t)$ will evolve according to the stochastic differential equation

$$\partial_t f = D_s \partial_x^2 f + \bar{s} f(1-f) - \bar{\mu} f + \sqrt{D_g f(1-f)}\,\xi, \quad (1)$$

where $\bar{s} = s/\tau_g$, $\bar{\mu} = \mu/\tau_g$, and $\xi \equiv \xi(x,t)$ is a Gaussian, white spatio-temporal noise with zero mean, $\langle \xi(x,t) \rangle = 0$, and unit variance: $\langle \xi(x,t)\xi(x',t') \rangle = \delta(t'-t)\delta(x'-x)$. The noise is interpreted in the Itô sense [17] and describes the stochastic birth-death processes of the cells at the frontier, which have some effective genetic drift strength $D_g$. We have the scaling $D_g \sim \ell/N\tau_g$, where $\ell$ is the linear size of the frontier over which cells compete to divide into virgin territory (approximately a cell diameter), and $N$ is the number of these competing cells. The diffusion term $D_s\partial_x^2 f$ describes cell rearrangements at the frontier with an effective spatial diffusion constant $D_s$. The parameters $D_s$ and $D_g$ will depend on the details of the microbial colony structure such as the nutrient penetration depth. They are measured for various microbial colonies in Refs. [11, 18]. We will be primarily interested in how various solutions to Eq. (1) depend on $\mu$ and $s$, which we can control in the experiment.

Equation (1) belongs to the directed percolation universality class and exhibits the associated non-equilibrium phase transition [7]. The transition can be found by examining sectors of unconverted cells as in Fig. 1(b) (i.e., by using Eq. (1) to evolve an initial $f(x, t = 0)$ with a localized "spike" of blue cells at the origin), but a uniform initial condition also exhibits a phase transition along the same phase boundary [8, 19]. Namely, if we start with all blue cells at the initial frontier ($f(x, t = 0) = 1$), the average fraction of blue cells $\langle f(x,t) \rangle_x$ (averaged over the noise $\xi$ in Eq. (1) and positions $x$ along the frontier), will approach a non-zero constant $\langle f(x,t) \rangle_x \to f_\infty > 0$ as $t \to \infty$ in the active phase and $\langle f(x,t) \rangle_x \to 0$ in the inactive phase. We will explore this initial condition using yeast range expansions in the next section.

The directed percolation phase transition line occurs at approximately $\mu \approx As^2$ for the range expansions, compared to $\mu \sim s$ for well-mixed populations, where $A$ is a constant of proportionality that will depend on $D_s$ and $D_g$. We expect the noise term $D_g$ to be important near the conversional meltdown transition. Then, in the strong noise limit, the following scaling should hold: $A \sim D_s/(D_g^2\tau_g)$ [8, 20]. Using the results of Ref. [18], we expect $A \approx 6$. However, our growth conditions and yeast strains are different and a detailed check of the scaling of $A$ with $D_s$ and $D_g$ is beyond the scope of this paper. So, we will use $A$ as a fitting parameter in the experimental results.

It is also possible to make some predictions for the sector angles illustrated in Fig. 1(a) using properties of the directed percolation universality class. First, note that a genetic sector formed from an unconverted (blue) cell at the frontier will have an opening angle $\theta$ given by

$$\theta = 2 \arctan\left[\frac{\xi_\perp}{\xi_\parallel}\right], \quad (2)$$

where $\xi_\perp/\xi_\parallel$ is the slope of the sector boundaries. The

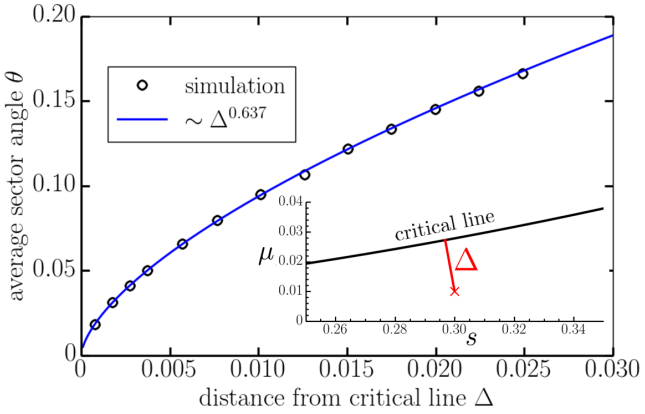


FIG. 3. Average sector angles measured from 25600 simulations of two-dimensional range expansions as a function of the distance $\Delta$ away from the critical line separating the active and inactive phases shown in Fig. 1(b). The inset illustrates the distance $\Delta$ and the critical line. In the simulations, the distance $\Delta$ is varied by fixing $s = 0.3$ and varying the mutation rate $\mu$. The range expansion has a flat frontier of 4000 cells and is evolved for $4 \times 10^4$ generations. We initialize the populations with a single unconverted cell at the frontier and average the opening sector angle of all surviving sectors.

opening angle can be measured in experiment. Note that we will only get a surviving sector if we are in the active phase (see Fig. 1(b)), where there is a non-zero probability that the unconverted cell type will survive at long times. Then, consider points $(s, \mu)$ in the phase diagram that are some shortest distance $\Delta \equiv \Delta(s, \mu)$ away from the phase transition line. We know that as we approach the phase transition line and $\Delta \to 0^+$, the dynamics will be governed by directed percolation. In particular, the slope $\xi_\perp/\xi_\parallel$ of the sector (measured relative to the population frontier) will be proportional to a power law of $\Delta$:

$$\frac{\xi_\perp}{\xi_\parallel} = a_\xi \Delta^{\nu_\perp (z-1)}, \tag{3}$$

where $a_\xi$ is a constant of proportionality, $z \approx 1.581$ is a dynamical critical exponent, and $\nu_\perp \approx 1.097$ is a spatial correlation length exponent [19]. The constant of proportionality $a_\xi$ is not universal and will depend on where we are along the transition line and particular details of our model. So, in summary, as long as we are close to the transition and the angle $\theta$ is small,

$$\theta \approx 2 \arctan \left[ a_\xi(s) \Delta^{\nu(z-1)} \right] \approx 2 a_\xi \Delta^{0.637}. \tag{4}$$

The prediction in Eq. (4) may be checked with simulations. We simulate range expansions with flat, uniform frontiers on a triangular lattice with a single cell per lattice site. The frontiers are a single cell wide and correspond to rows of the lattice. Cells at the frontier compete with their neighbors to divide into the next lattice row. The probability of division is proportional to the cell growth rate. The unconverted blue cells have a growth rate normalized to 1, while the converted yellow cells grow with rate $1 - s$. This implements the selective advantage of the blue cells. After a cell division, the daughter cell may mutate with probability $\mu$ if it is unconverted (just as in the designed yeast strain). These competition rules are a generalization of the Domany-Kinzel model updates [21]. The model implementation is described in detail in Ref. [8]. It is possible to evolve sectors by considering initial frontiers with just a single blue cell surrounded by all yellow cells. Some examples of the resulting sectors are shown in the insets of Fig. 1(b). We then measure the average angle $\theta$ subtended by the blue cell sectors as a function of the distance $\Delta$ away from the extinction transition line in the $(\mu, s)$ plane (see inset of Fig. 3). We find excellent agreement between simulation and Eq. (4) in Fig. 3. The parameter $a_\xi \approx 0.88$ is found by fitting. We will check these results with experiments in the next section.

## EXPERIMENTAL RESULTS

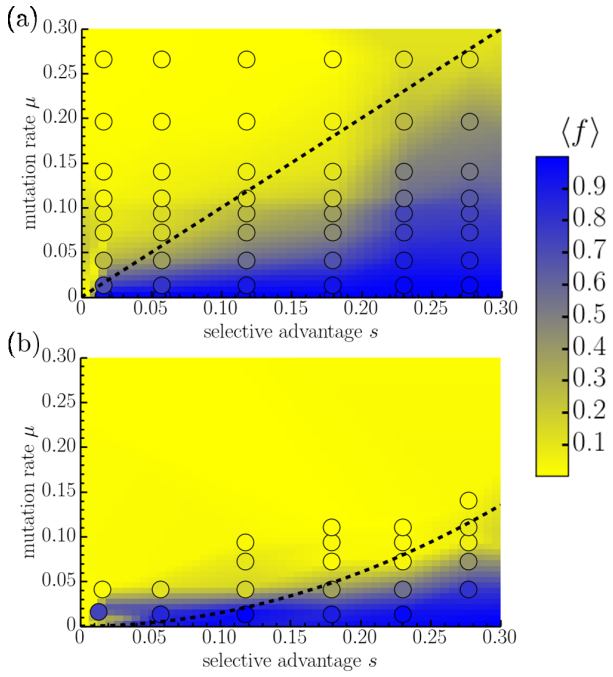


FIG. 4. The average steady-state fraction of unconverted cells $\langle f \rangle$ in (a) well-mixed populations cultured in a test-tube and in (b) range expansions. The concentration for the range expansions was measured by sampling cells at the edge of a circular colony after five days of growth. The dashed lines are the theoretical predictions of the phase transition lines. In (a), we expect that the transition occurs around $\mu \approx s$. In (b), we get the significantly different line shape $\mu \approx A s^2$, with $A \approx 1.5$ as the single parameter fit to the data.

We first compare the steady-state concentration of un-

converted blue cells in well-mixed populations and two-dimensional range expansions as a function of the mutation rate $\mu$ and the blue cell selective advantage $s$. We expect that if $\mu$ is large enough compared to $s$, the fit blue strain is unable to survive in the population at long times. Thus, we expect the average fraction of blue cells $\langle f \rangle$ to eventually decay to zero. Otherwise, the fraction will approach some non-zero steady-state value $f_\infty$. We estimate this value in the well-mixed populations by measuring the fraction of mCherry-expressing unconverted cells by flow cytometry after enough generations to achieve a steady-state (approximately 40, or four thousand-fold dilutions from saturation) or until the unconverted fraction is no longer measurable. Similarly, we estimate the fraction of unconverted cells in colonies at steady-state by collecting cells from the very edge of circular colonies after five days' growth with a pipette tip and performing flow cytometry. The population frontier inflates in the circular range expansions, which has consequences for the dynamics. However, the steady-state fraction $f_\infty$ does not change much [8].

The experimental results in Fig. 4 vividly illustrate the effects of spatial fluctuations on the transition to extinction. We see that there is a much smaller section of the $(\mu, s)$ space that yields a non-zero steady-state fraction of unconverted cells in the population. The theoretical predictions for the phase boundaries are consistent with the experiment: We find $\mu \approx s$ for the well-mixed population and $\mu \approx A\, s^2$ for the populations grown on Petri dishes, where $A \approx 1.5$ is a fitting parameter. Note that $A$ is a number of order unity, as we expected from the scaling argument $A \sim D_s/D_g^2\tau_g$.

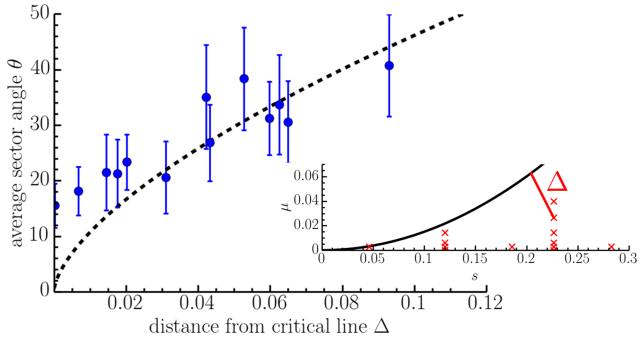


FIG. 5. Measured averages of opening angles of sectors formed in experimental linear range expansions as a function of the distance $\Delta$ from the critical line found in Fig. 4(b). The dashed line shows the fit to the expected directed percolation power law behavior in Eq. (4). Inset: The black lines shows the position of the transition. The red crosses show the $(\mu, s)$ coordinates of all the growth conditions used to grow the colonies in the experiment. The distance $\Delta$ is also shown for one of these points with a solid red line.

It is also interesting to study the opening angle $\theta$ formed by the sectors in linear range expansions as we approach the phase transition line. From Eq. (4), we expect this angle to vanish as a power-law with decreasing distance $\Delta$ from the critical line (see inset of Fig. 3). The measured opening angles as a function of $\Delta$ are shown in Fig. 5. The values are collected by approximating the opening sector angle from images of the colony edges and averaging over many sectors. The error bars are calculated from the standard deviations of the sector angle measurements used to compute the averages. Growth conditions corresponding to many different values of $\mu$ and $s$ were used, as illustrated in the inset of Fig. 5. We see that the theoretical prediction gives reasonable results, except for small $\Delta$. This is expected because the colony sector angle vanishes as $\Delta \to 0$ and the smaller sectors are harder to identify in the range expansion images. We also expect some error due to the variation of the non-universal parameter $a_\xi$ along the transition line (see Eq. (4)).

## CONCLUSION

We have now examined an extinction transition using a genetically modified yeast strain that irreversibly converts from a more to a less fit strain. This synthetic strain maintains many sources of biological variability, including variability in growth rate/orientation, while providing exquisite control over conversion, relative growth rate, and visualization of two cell types. Experiments with this strain thus provide an appropriate validation for the analytical and simulation-based approaches presented in this work.

The effects of spatial dynamics on the transition have been clearly demonstrated. We found that spatial fluctuations enhance extinction through genetic drift: The extinction in a well-mixed population occurs when $\mu \sim s$ and when $\mu \sim s^2$ for a range expansion with a thin (approximately one-dimensional) frontier. Hence, the unconverted strain is maintained in a smaller region of the $(\mu, s)$ phase space in the range expansion compared to the well-mixed case, as shown in Fig. 4. We expect that this enhancement is generic. The enhanced extinction probability might be observable in other spatially structured populations, such as tissue growth and natural range expansions. The enhanced extinction probability has important implications for pathological conditions and cancer.

We also looked at the opening sector angles of clusters of the fit strain spreading through a less fit population. The opening angle vanishes with a directed percolation power law as we approach the extinction transition. We have verified this power law with both simulations and experiments. Such sector dynamics might be relevant for cancer, where driver mutations may spread through an otherwise slowly-growing cancerous population while ac-

cumulating irreversible, deleterious mutations [22]. Even when many deleterious mutations accumulate, we expect that there is an analogous extinction transition at which the mutations accumulate fast enough to lead to a population collapse of the cells with the driver mutation [22, 23].

To better understand these dynamics in cancer, we would need to consider three-dimensional range expansions with effectively two-dimensional frontiers, such as the surfaces of solid tumors. In three-dimensional populations, the extinction dynamics may be quite different [23]. Spatial fluctuations do not enhance genetic drift as much, and the phase diagram for extinction will have a different shape. It would be interesting to examine three-dimensional range expansions of this synthetic strain to look at how these different spatial dynamics influence the extinction transition. This may be done by embedding the yeast in soft agar, or growing them in cylindrical columns with nutrients supplied at one end, as described in Ref. [24].

We thank Bryan Weinstein for helpful discussions. This work was supported by the National Science Foundation (NSF) through grant DMR-1306367, by the NIH through NIGMS grant GM068763, and by the Harvard Materials Research Science and Engineering Center (DMR-1420570). MOL also acknowledges support from NSF grant DMR-1262047. MEW was supported by the NDSEG and NSF GRFP fellowships. We thank Derek Lindstrom and Dan Gottschling for generously providing their inducible Cre construct $P_{SCW11}$*cre-EBD78*. The computer simulations were run on the Odyssey cluster, maintained by the Harvard University Research Computing Group.

* lavrentm@gmail.com

[1] I. L. Weissman, Cell **100**, 157 (2000).
[2] J. J. Bull and E. L. Charnov, Evolution **39**, 1149 (1985).
[3] B. D. Simons and H. Clevers, Exp. Cell. Res. **317**, 2719 (2011).
[4] S. J. Morrison and A. C. Spradling, Cell **132**, 598 (2008).
[5] H. J. Muller, Mutat. Res.-Fund. Mol. M. **1**, 2 (1964).
[6] L. Chao, Nature **348**, 454 (1990).
[7] H. Hinrichsen, Adv. in Phys. **49**, 815 (2000).
[8] M. O. Lavrentovich, K. S. Korolev, and D. R. Nelson, Phys. Rev. E **87** (2013).
[9] H. J. Snippert, L. G. van der Flier, T. Sato, J. H. van Es, M. van den Born, C. Kroon-Veenboer, N. Barker, A. M. Klein, J. van Rheenen, B. D. Simons, et al., Cell **143**, 134 (2010).
[10] K. S. Korolev, M. Avlund, O. Hallatschek, and D. R. Nelson, Rev. Mod. Phys. **82**, 1691 (2010).
[11] K. S. Korolev, J. B. Xavier, D. R. Nelson, and K. R. Foster, The American Naturalist **178**, 538 (2011).
[12] K. S. Korolev, M. J. I. Müller, N. Karohan, A. W. Murray, O. Hallatschek, and D. R. Nelson, Phys. Biol. **9**, 026008 (2012).
[13] M. O. Lavrentovich, J. H. Koschwanez, and D. R. Nelson, Phys. Rev. E **87**, 062703 (2013).
[14] M. E. Wahl and A. W. Murray, bioRxiv (2015), doi:10.1101/010728.
[15] D. L. Lindstrom and D. E. Gottschling, Genetics **183**, 413 (2009).
[16] W. Stöcklein, W. Piepersburg, and A. Böck, FEBS Lett. **136**, 265 (1981).
[17] C. W. Gardiner, *Handbook of Stochastic Methods* (Springer-Verlag, Berlin, 1985), 2nd ed.
[18] M. J. I. Müller, B. I. Neugeborn, D. R. Nelson, and A. W. Murray, Proc. Nat. Acad. Sci. **111**, 1037 (2014).
[19] M. Henkel, H. Hinrichsen, and S. Lübeck, *Non-Equilibrium Phase Transitions*, vol. I - Absorbing Phase Transitions (Springer Science, The Netherlands, 2008).
[20] C. R. Doering, C. Mueller, and P. Smereka, Physica A **325**, 243 (2003).
[21] E. Domany and W. Kinzel, Phys. Rev. Lett. **53**, 311 (1984).
[22] C. D. McFarland, K. S. Korolev, G. V. Kryukov, S. R. Sunyaev, and L. A. Mirny, Proc. Nat. Acad. Sci. **110**, 2910 (2013).
[23] M. O. Lavrentovich, J. Stat. Mech. **2015**, P05027 (2015).
[24] C. Vulin, J.-M. D. Meglio, A. B. Lindner, A. Daerr, A. Murray, and P. Hersen, Biophys. J. **106**, 2214 (2014).